Development 139, 1296-1305 (2012) doi:10.1242/dev.078238

2-O-sulfotransferase regulates Wnt signaling, cell adhesion and cell cycle during zebrafish epiboly

Erin L. Cadwalader, Maureen L. Condic and H. Joseph Yost*

SUMMARY

O-sulfotransferases modify heparan sulfate proteoglycans (HSPGs) by catalyzing the transfer of a sulfate to a specific position on heparan sulfate glycosaminoglycan (GAG) chains. Although the roles of specific HSPG modifications have been described in cell culture and invertebrates, little is known about their functions or abilities to modulate specific cell signaling pathways in vertebrate development. Here, we report that 2-O-sulfotransferase (2-OST) is an essential component of canonical Wnt signaling in zebrafish development. 2-OST-defecient embryos have reduced GAG chain sulfation and are refractory to exogenous Wnt8 overexpression. Embryos in which maternally encoded 2-OST is knocked down have normal activation of several zygotic mesoderm, endoderm and ectoderm patterning genes, but have decreased deep cell adhesion and fail to initiate epiboly, which can be rescued by re-expression of 2-OST protein. Reduced cell adhesion and altered cell cycle regulation in 2-OST-deficient embryos are associated with decreased β-catenin and E-cadherin protein levels at cell junctions, and these defects can be rescued by reactivation of the intracellular Wnt pathway, utilizing stabilized β-catenin or dominant-negative Gsk3, but not by overexpression of Wnt8 ligand. Together, these results indicate that 2-OST functions within the Wnt pathway, downstream of Wnt ligand signaling and upstream of Gsk3β and β-catenin intracellular localization and function.

KEY WORDS: Wnt signaling, HSPG, Epiboly, Gastrulation, Zebrafish

INTRODUCTION

Heparan sulfate proteoglycans (HSPGs) are a family of cell surface and extracellular matrix proteins with glycosaminoglycan (GAG) chains covalently attached to a protein core. Many types of cell behavior are thought to be modulated by HSPGs, from self-renewal and adhesion to differentiation and migration (Esko and Selleck, 2002; Hacker et al., 2005; Lamanna et al., 2007). The ability of HSPGs to modulate cellular responses is partially controlled by modifications to the GAG chains (Gotte et al., 2008; Reijmers et al., 2010; Reim and Brand, 2006; Walsh and Stainier, 2001).

The GAG chains present in HSPGs are disaccharide repeats, 50-100 units in length on average, composed of alternating glucuronic acid and N-acetyl-glucosamine (Esko and Selleck, 2002). Modifications to these GAG chains by several different families of enzymes epimerize ring structures, add sulfates and remove acetylases in a non-template-driven fashion, resulting in variable regions of sulfation on each GAG chain and creating an astonishing level of complexity within one cell-surface HSPG. Gene knockdown and mutants for HSPG core proteins and modifying enzymes have developmental defects that suggest distinct roles for HSPGs with specific modifications, but none of these studies has identified sulfation-dependent signaling pathways in early development (Bink et al., 2003; Bullock et al., 1998; Fujita et al., 2010; Habuchi et al., 2007; Kamimura et al., 2004).

In this study, we focus on one GAG modifying enzyme, 2-O-sulfotransferase (2-OST). 2-OST catalyzes the transfer of a sulfate from a phosphate donor, 3′-phosphoadenosine 5′-phosphosulfate (PAPS), to the second carbon position on the glucuronic acid of the disaccharide chains. Studies in mice and worms previously demonstrated a role for 2-O-sulfation in cell migration and differentiation through unknown pathways (Bullock et al., 1998; Kinnunen et al., 2005).

The zebrafish begins as a single cell atop a yolk mass, undergoing several rounds of synchronous cell division to form a blastodisc (Kimmel et al., 1995; Kimmel and Law, 1985b). At 4 hours post-fertilization (hpf), the process of epiboly begins. At this time, the most superficial layer of epithelium, the enveloping layer (EVL), begins a downward migration towards the vegetal pole. The EVL gradually surrounds the yolk and epiboly concludes with complete enclosure of the yolk cell (Betchaku and Trinkaus, 1978; Kane and Adams, 2002). The cells of the blastodisc beneath the EVL, known as the deep cells, give rise to the embryo proper through a variety of cell movements during gastrulation (Rohde and Heisenberg, 2007). These embryonic deep cells intercalate and expand vegetally, filling the space between the EVL and the non-embryonic yolk during the epiboly movements (Kane et al., 2005). The extent to which epiboly is driven by forces pulling the EVL downwards compared with the expansion forces of the deep cells is still unclear.

Here, we examine the role of 2-OST (*hs2st1a* – Zebrafish Information Network) in cell migration, adhesion and proliferation in zebrafish embryos, and show that the canonical Wnt pathway is dependent on 2-OST function. We show that reducing 2-OST levels in zebrafish results in a failure to initiate epiboly. At the cellular level, β-catenin and E-cadherin protein localization and intracellular level are altered, resulting in reduced cell adhesion within the embryonic deep cells and altered cell cycle regulation. Results from a series of epistasis experiments indicate that cellular effects in 2-OST-deficient embryos can be rescued by reactivation of the intracellular canonical Wnt pathway. These results demonstrate that 2-OST function is required for normal Wnt signaling in embryonic cells during epiboly initiation.

Department of Neurobiology and Anatomy, Eccles Institute of Human Genetics, University of Utah, Salt Lake City, UT 84112, USA.

*Author for correspondence (jyost@genetics.utah.edu)

Accepted 8 January 2012

MATERIALS AND METHODS

Zebrafish lines

Oregon AB wild-type zebrafish (*Danio rerio*) and the transgenic line *Tg(TOP:GFP)w25*, courtesy of Rich Dorsky (University of Utah, UT, USA), were maintained on a 14 hour light/10 hour dark cycle at 28.5°C. Zebrafish embryos resulted from natural spawning and were collected, injected, raised and staged as previously described (Essner et al., 2005; Westerfield, 1993).

Morpholino and RNA injection of zebrafish embryos

The following morpholino oligonucleotides (MOs) were used: 2-OST MO1 (5′-TGACCGAGAACTTTATTACACACAG-3′), 2-OST MO2 (5′-AAGCCCCATCAAAAAATCCAGCAGG-3′) and, as a control, 3-OST-7 MO (5′-CACATAACTCAGAAGATTGGCCATG-3′). The first 2-OST-specific MO (2-OST MO1) targeted the sequence directly upstream of the translation initiation site. The second 2-OST-specific MO (2-OST MO2) recognized the region surrounding the translation start site, not overlapping the first MO. Embryos were injected at the 1- to 2-cell stage. For the rescue of the 2-OST MO1 phenotype, 200 pg of *2-ost* mRNA (GenBank Accession number DQ812997.1) with a β-globin 5′ UTR, instead of the endogenous *2-ost* 5′ region, was co-injected with the morpholino. Owing to the altered 5′ region, the 2-OST MO1 cannot bind the rescue RNA. The *2-ost* mRNA was cloned out of the pBSII T7 vector and into a modified pCS2+ expression vector using the *Nco*I and *Xba*I restriction enzymes. β-*galactosidase* mRNA was injected as a control (GenBank Accession number AP_000996). pCS2+-stabilized β-catenin and pT7T-Wnt8 expression vectors were gifts from Rich Dorsky. The *Xenopus* pCS2+-dnGSK3 expression vector was a gift from Monica Vetter (University of Utah, UT, USA). RNA was made using respective Message Machine kits (Ambion).

^{35}S radiolabeling

Embryos were injected with morpholino at 1- to 2-cell stage. At 3.5 hpf, ^{35}S was injected into the yolk. The embryos were grown at room temperature for five hours. Only viable embryos were then collected, an average of 90 embryos per group, in PBS and Pronase solution, and incubated overnight. GAG chains were isolated in a series of steps requiring 0.2 μm syringe filtration to remove all course particulate from the overnight digest, DEAE-Sephacel column filtration to separate the hot GAG chains, and PD10 desalting columns to remove the high levels of salt from the solution, which had been used to elute the GAG chains in the previous step (Lawrence et al., 2008). A liquid scintillation counter (Beckman Coulter LS6500) was used to determine the rate of incorporation for each sample after each step. To determine the percentage of incorporation of ^{35}S, the counts per unit (cpu) levels after the last step were compared with the cpu levels after the 0.2 μm filtration steps, the average per embryo calculated, and these levels were normalized to the wild type.

In situ hybridization

For in situ hybridization analysis, embryos were fixed overnight at 4°C in sucrose-buffered 4% paraformaldehyde. They were subsequently rinsed in phosphate buffered saline (PBS), dehydrated in methanol, and stored at –20°C. Clones encoding the open reading frame (ORF) of *goosecoid*, *sonic hedgehog*, *eve1*, *sox17*, *no tail*, *lefty2*, *lcp1* (a gift from Mike Redd, University of Utah, UT, USA) and *gata6* were used to make probes via in vitro transcription. Antisense RNA was made from those linearized plasmids using Digoxigenin (DIG) RNA Labeling Kit (Roche, IN, USA). In situ hybridizations were carried out according to a previously established protocol (Essner et al., 2000) using a Biolane HTI in situ machine (Huller and Huttner AG, Tübingen, Germany). Embryos were cleared in 70% glycerol in PBST and photographed with a Nikon SMZ1000 on a Leica MZ12 dissecting microscope. Digital images were processed using Adobe Photoshop and ACD systems Canvas.

Immunohistochemistry

Immunohistochemical analysis for proteins was performed on embryos fixed overnight at room temperature in 4% paraformaldehyde. They were subsequently rinsed in PBST, dechorionated, and blocked for one hour in blocking solution (1% DMSO, 5% goat serum, 5% Triton X-100 in PBS). They were blocked overnight in parallel using aliquots from a primary antibody in blocking solution. They were then washed with blocking solution and subsequently incubated overnight in secondary antibody. The following primary antibodies and dilutions were used: rabbit anti-β-catenin (Sigma, 1:300), mouse anti-E-cadherin (BD Bioscience, 1:100), rabbit anti-phospho-histone 3 (Santa Cruz, 1:500), mouse anti-BrdU (Sigma, 1:500). Sytox Green was used as a nuclear stain (Invitrogen, 1:100). Alexa 488 donkey anti-rabbit, Alexa 546 donkey anti-rabbit, and Alexa 647 goat anti-mouse were used as secondary antibodies (Invitrogen, 1:200). Embryos were mounted in Slow Fade (Invitrogen) on cover slips and visualized using Olympus FV300 XY. Images were analyzed using ImageJ and MetaMorph software. The 20× image intensity levels were unmodified and all processed in parallel. The brightness and contrast of 60× images were increased in 2-OST morphants to highlight morphological differences.

For the cell counting experiments, cell division was cold arrested, then BrdU analog was injected into the yolk of the cold embryos and allowed to diffuse for half an hour in the cold before embryos were restored to the incubator and allowed to resume growth for half an hour, at which point they were fixed in 4% PFA in PBS. They were then processed as described above, with the addition of an incubation step (20 minutes) in 2 M HCl.

Western blot

Wild-type and injected embryos were manually dechorionated, the animal caps were manually removed from the yolk, the caps were collected in lysis buffer, and western blots were performed as previously described (Link et al., 2006). Primary antibodies used were mouse anti-α-tubulin (AbCam, 1:7500) as a control, rabbit anti-β-catenin (Sigma, 1:2000), mouse anti-E-cadherin (Anaspec, 1:2000), rabbit anti-active β-catenin (Millipore, 1:500) and rabbit anti-HS2ST (AbCam, 1:500). Secondary antibodies used were HRP-conjugated goat anti-mouse and HRP-conjugated goat anti-rabbit (Jackson ImmunoResearch, 1:2000). Membranes were exposed using ECL+ Western Blotting Detection System (Amersham). Densitometry analysis was performed using AlphaEase FC.

Quantitative real-time PCR

Wild-type and injected embryos were collected in Trizol at 4 hpf in triplicate bioassay series, RNA was isolated with chloroform extraction and RNA was further purified after DNAse treatment using RNEasy columns (Qiagen). RNA was quantified and equal amounts of RNA were used in conjunction with oligo(dT) to make cDNA using Superscript III RT-PCR Kit (Invitrogen). Quantitative PCR was performed using PerfeCTa SYBR Green SuperMix (Quanta Biosciences) on an iCycler thermal cycler (BioRad) with iCycler software. *gapdh*, *axin2*, *dkk1b* and enhanced green fluorescent protein (EGFP) primers were optimized for efficiency and used for the amplifications. Results were analyzed using the ΔΔcT method.

Statistics

Statistical significance was analyzed using Student's *t*-test. Analysis was carried out by R-Commander software package within the R Statistical Software platform. Results are considered significant when $P<0.05$ and results are expressed as mean ± s.d.

RESULTS

Epiboly initiation requires 2-O-sulfation

2-ost mRNA is maternally deposited and ubiquitously expressed through gastrulation (Cadwallader and Yost, 2007). To address the roles of 2-OST in early development, two different translation blocking (AUG) MOs were injected at the 1- to 2-cell stage, to reduce protein expression from maternal *2-ost* mRNA. As a control for morpholino injection effects, an AUG MO against another ubiquitously expressed GAG chain modifying enzyme, 3-O-sulfotransferase-7, was injected in parallel. The control morphants progressed through the initiation of epiboly and through gastrulation normally, displaying normal embryonic phenotypes (Fig. 1A-C). Embryos injected with either 2-OST MO1 or 2-OST MO2 developed normally up to the point of epiboly initiation (Fig. 1D,E,G,H). However, at the onset of epiboly, EVL cells failed to

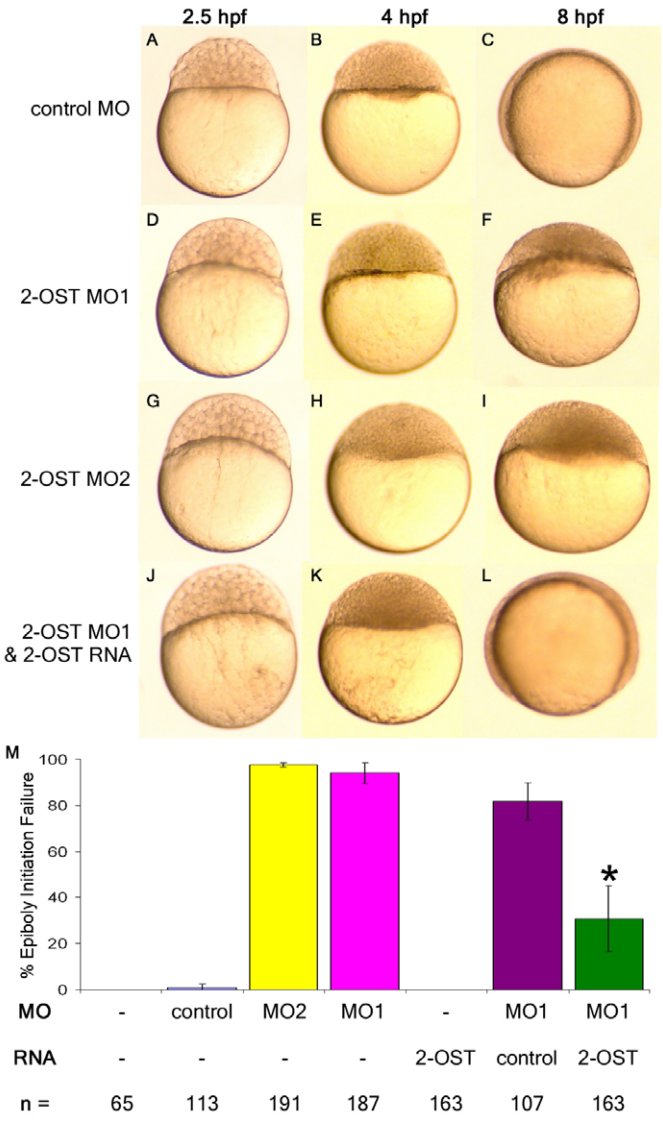

Fig. 1. 2-OST is necessary for epiboly in early zebrafish development. (**A-L**) Embryos (1- to 2-cell stage) were injected with 3 ng control MO (A-C), 3 ng of 2-OST MO1 (D-F), 3 ng of 2-OST MO2 (G-I), or mixture of 3 ng 2-OST MO1 and 0.2 ng 2-OST RNA (J-L), then incubated in embryo water at 28°C. They were examined at 2.5 hpf (A,D,G,J), 4 hpf (B,E,H,K) and 8 hpf (C,F,I,L). (**M**) Quantitative comparison of injections and rescue scored based on failure to initiate epiboly. The co-injection of 2-OST MO+2-OST RNA rescued the percentage of embryos that fail to initiate epiboly in the 2-OST MO alone or the 2-OST MO+control RNA by >50%. *P<0.05. Error bars represent s.d.

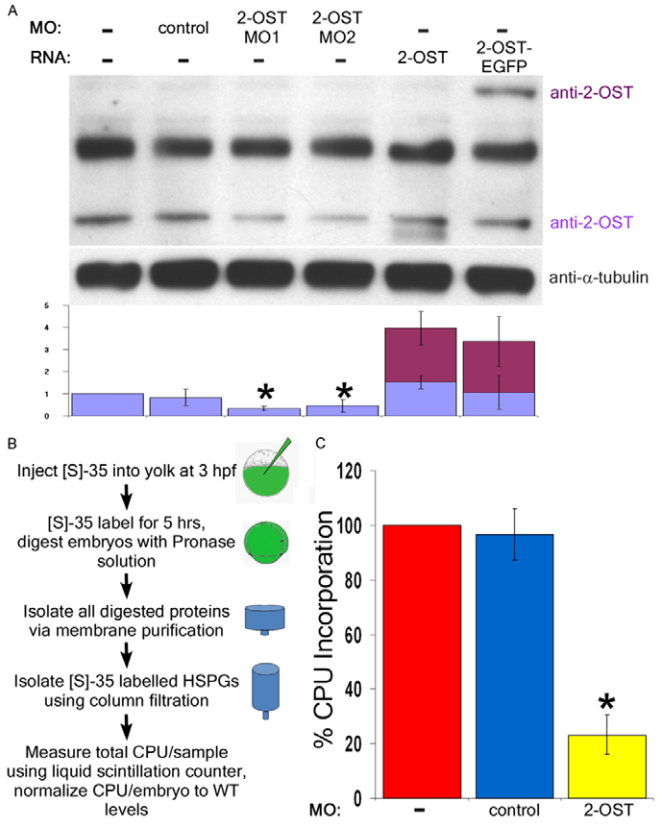

Fig. 2. 2-OST morphants display reduced levels of 2-OST protein and reduced levels of ^{35}S incorporation. (**A**) By western blot, levels of 2-OST protein were shown to be statistically significantly reduced by roughly half using both 2-OST MO1 and MO2 compared with WT and control embryos at 4 hpf. The antibody was validated using 2-OST RNA, with degradation product or altered post-translational modifications beneath the band, and 2-OST-EGFP RNA (two embryos/lane/sample, n=4 experiments). Quantification of protein levels was normalized to uninjected levels of 2-OST relative to the total levels of α-tubulin per sample. (**B**) WT, control MO and 2-OST MO embryos were injected with 1 nl 10 mCi ^{35}S, grown for five hours, and collected at 8 hpf (n=3, 90 embryos group/n). Protein purification was performed to isolate radiolabeled GAG chains and cpu per embryo was calculated based on liquid scintillation counting results. (**C**) Ratio of ^{35}S incorporation per embryo was normalized to WT. The 2-OST morphants exhibit a nearly 80% decreased rate of incorporation of ^{35}S compared with WT and control morphants. *P<0.05. Error bars represent s.d.

initiate migration in the vegetal direction, resulting in cells remaining atop the yolk cell (Fig. 1F,I). 2-OST morphants exploded at ~10 hpf, apparently by aberrant contraction in the yolk at the margin of the blastodisc and lysis of the yolk cell (supplementary material Movie 1).

As an important control for morpholino specificity and off-target effects, we found that the epiboly initiation defect in 2-OST morphants can be rescued by co-injection of mRNA encoding 2-OST protein which does not have the same 5′UTR as the endogenous *2-ost* gene, thereby preventing the MO from binding this RNA sequence. Embryos injected with 2-OST MO1 and 200 pg *2-ost* rescue mRNA initiated epiboly in parallel with control morphants and proceeded through gastrulation, resulting in apparently normal embryos at 24 hpf (Fig. 1J-M). Injection of 200 pg of *2-ost* rescue mRNA alone caused no apparent overexpression phenotype, and 200 pg of control mRNA was not able to rescue the 2-OST morphant phenotype. These results indicate that 2-OST is required for epiboly.

2-OST protein and 2-O-sulfation levels reduced in 2-OST morphants

To determine whether the 2-OST morpholinos altered the levels of 2-OST protein prior to the stage at which the defect first manifests, we performed western blot analysis of embryos at 4 hpf, comparing the levels of 2-OST protein in wild-type uninjected (WT) embryos, control morphant-injected embryos and both 2-OST-MO1 and 2-OST-MO2 morpholino-injected embryos (Fig. 2A). The antibody recognized a 42 kDa band of the predicted size of 2-OST, and a

prominent, non-specific band at 55 kDa (Fig. 2A). Because this antibody had not been validated in zebrafish, we also injected embryos with mRNA in which the 2-OST coding region is fused in-frame to GFP, generating a larger 2-OST protein that could be detected as a discrete band at 69 kDa by western blot analysis. The 2-OST protein levels were normalized to the levels of tubulin for each sample, and then the total levels of 2-OST in each sample were compared with WT levels. From these experiments, we observed that the 2-OST protein levels in the 2-OST morphants were approximately half the levels observed in uninjected controls or in embryos injected with control morpholino.

To determine whether morpholino knockdown of 2-OST results in a reduction of the levels of sulfation of GAG chains, WT embryos, control morphants and 2-OST morphants were pulse-labeled with ^{35}S radionuclide. A variety of GAG-chain radio-labeling methods were tested, including soaking embryos in their chorions in organic ^{35}S, manually dechorionating embryos before soaking in ^{35}S, microinjection of ^{35}S into the chorionic space, and microinjection into the yolk cell. The most effective approach was found to be microinjection of ^{35}S directly into the yolk at 3 hpf, and allowing label incorporation into the biosynthetic pathway for GAG chain sulfation for 5 hours (Fig. 2B). Thus, after morpholino injection at the 1- to 2-cell stage and injection of ^{35}S directly into the yolk at 3 hpf, viable embryos were collected at 8 hpf, with equal numbers of embryos from each group (255 embryos/group, n=3). The levels of ^{35}S incorporation into GAG chains were calculated by comparing the amount of radiolabel incorporation per embryo in the final step of the purification to the levels of total ^{35}S after the first digestion and purification, with the level for each sample normalized to WT embryos (Fig. 2B; supplementary material Table S1C). Strikingly, GAG sulfation in 2-OST morphants was 20% that of WT and control morphants, indicating that 2-OST morpholino was able to knock down 2-OST activity by 80% during the stages preceding epiboly (Fig. 2C). These results, in combination with the *2-ost* RNA rescue experiments and reduced 2-OST protein levels measured by western blot, show that the epiboly initiation defect in zebrafish embryos is correlated with a decrease in 2-O-sulfation of GAG chains.

2-OST morphants establish germ layers and form axes

To explore whether the epiboly defect in 2-OST morphants was due to a general loss of zygotic transcription, loss of patterning genes or decreased cell viability, we performed in situ hybridization at 8 hpf with several zygotically expressed patterning and primary germ layer markers that are initiated post-midblastula transition. We examined mesoderm germ layer markers, including the dorsal marker *goosecoid* (*gsc*; Fig. 3A,B), the ventral marker *eve1* (Fig. 3C,D) and the dorsal midline marker *sonic hedgehog* (*shh*; Fig. 3E,F). *lefty2* (*lft2*) and *no tail* (*ntl*) are dorsal and marginal mesendoderm markers, respectively (Fig. 3G-J). *sox17* is a marker for both endoderm as well as the dorsal forerunner cells (DFC) (Fig. 3K,L). *lcp1* marks the EVL endoderm (Fig. 3M,N) and *gata6* indicates the yolk syncytial layer (YSL) (Fig. 3O,P).

All of these zygotic markers were activated in 2-OST morphants in appropriate embryonic locations. This indicates that embryonic axes and germ layer precursors are established, although the patterns of expression were altered as expected in epiboly-defective embryos. In addition, total RNA and protein levels at 8 hpf were comparable in WT and 2-OST morphants (supplementary material Table S1A,B). Transcription of *shh* and *sox17* does not begin until mid-gastrulation; therefore, the expression of these markers in 2-OST morphants indicates that development is not significantly delayed. Together, these results suggest that the defects in epiboly initiation appear to be due to specific defects in cell behavior, not issues of initial embryonic patterning, zygotic transcription, developmental arrest or embryonic lethality.

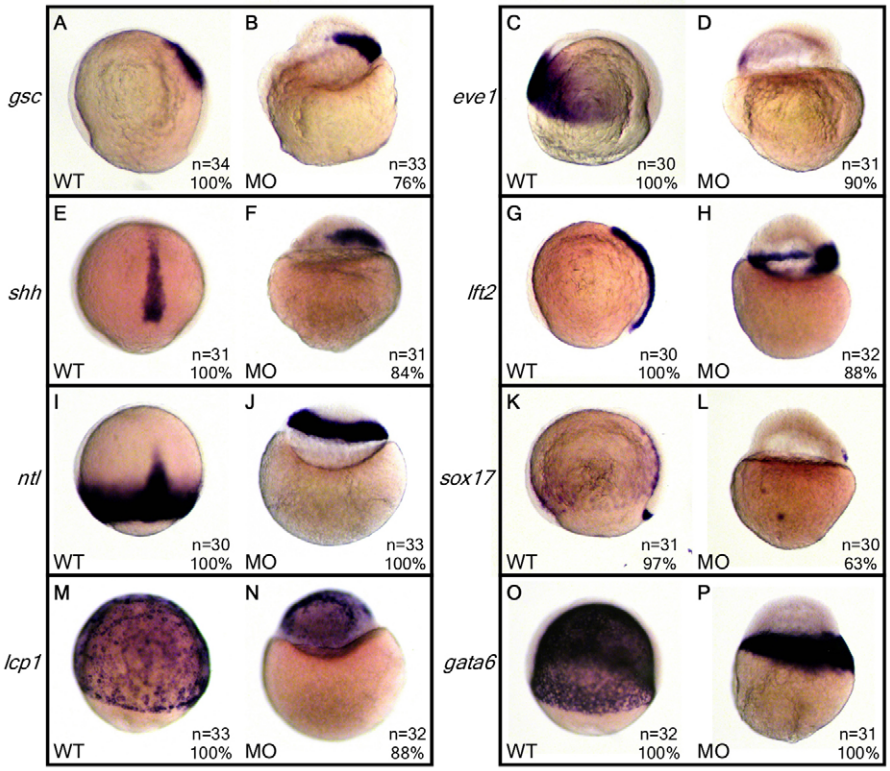

Fig. 3. Molecular marker expression in WT and 2-OST morphant embryos. (**A-P**) Wild-type embryos were injected with 3 ng of either control MO or 2-OST MO, fixed at 8 hpf, and processed for whole-mount in situ hybridization. Expression patterns of mesoderm markers (A-F), mesendoderm markers (G-J), a DFC and endoderm marker (K,L), an ectoderm marker (M,N) and a YSN marker (O,P) were analyzed. The presence and organization of these markers in both the WT and morphant embryos suggest that 2-OST morphants were establishing the primary germ layers and axes. Furthermore, the presence of *sox17* and *shh*, which are expressed later in development, indicate that the 2-OST morphants were not severely delayed in development.

2-OST is required for deep cell adhesion and membrane localization of β-catenin and E-cadherin

Previous studies revealed an important role for deep cells in the initiation of epiboly, with cell intercalations promoting the doming of the blastodisc over the yolk (Du et al., 2011). Loss of cadherin, a membrane-localized adherens junction protein, and corresponding alterations in deep cell morphology results in slowed or failed epiboly (Adachi et al., 2009; Babb and Marrs, 2004; Kane et al., 2005). Therefore, to assess whether the epiboly defects in 2-OST morphants are correlated with defects in cell morphology, adhesion and adherens junction localization in deep cells, we examined the accumulation and intracellular localization of the adherens junction proteins E-cadherin and β-catenin, by both confocal immunohistochemistry and western blot analyses at 4 hpf. WT embryos and control morphants had high levels of β-catenin (Fig. 4A,C, supplementary material Fig. S2A) and E-cadherin (Fig. 4B,C) protein localization at the cell membranes in the EVL and the deep cells. The cell shapes outlined by these epitopes were hexagonal, implicating strong levels of adhesion among the deep cells. By contrast, 2-OST morphants had decreased intensity of β-catenin (Fig. 4D,F) and E-cadherin (Fig. 4E,F) at the cell membranes in both the EVL and deep cells. In 2-OST morphants, cell morphologies were more rounded, suggesting decreased tension due to the reduced adhesion. Injection of 2-OST morpholino and lineage label into one cell in 32-cell embryos resulted in a similar phenotype in the morpholino-targeted lineages, with normal β-catenin at cell membranes in surrounding uninjected lineages, suggesting that the loss of β-catenin at the cell membranes was cell autonomous (supplementary material Fig. S1A-F). Additionally, gaps of variable sizes were present between the deep cells at a much greater frequency than was observed in the wild-type or control morphant embryos, indicating regions in which the cells had lost adherence to one another. Western blot analyses confirmed that the levels of β-catenin and E-cadherin protein accumulation were reduced in 2-OST morphants (Fig. 4M).

To assess more directly cell adhesion in zebrafish embryos, we surgically removed and cultured zebrafish animal cap cells from 4 hpf embryos. When animal cap cells were removed from WT animals, the sheet of cells remained intact in culture. By contrast, when the 2-OST morphant embryo animal caps were removed and cultured, deep cells immediately began to separate from the sheet of cells, indicating reduced cell adhesion. As an important control, this cell adhesion defect was rescued by the co-injection of the *2-*

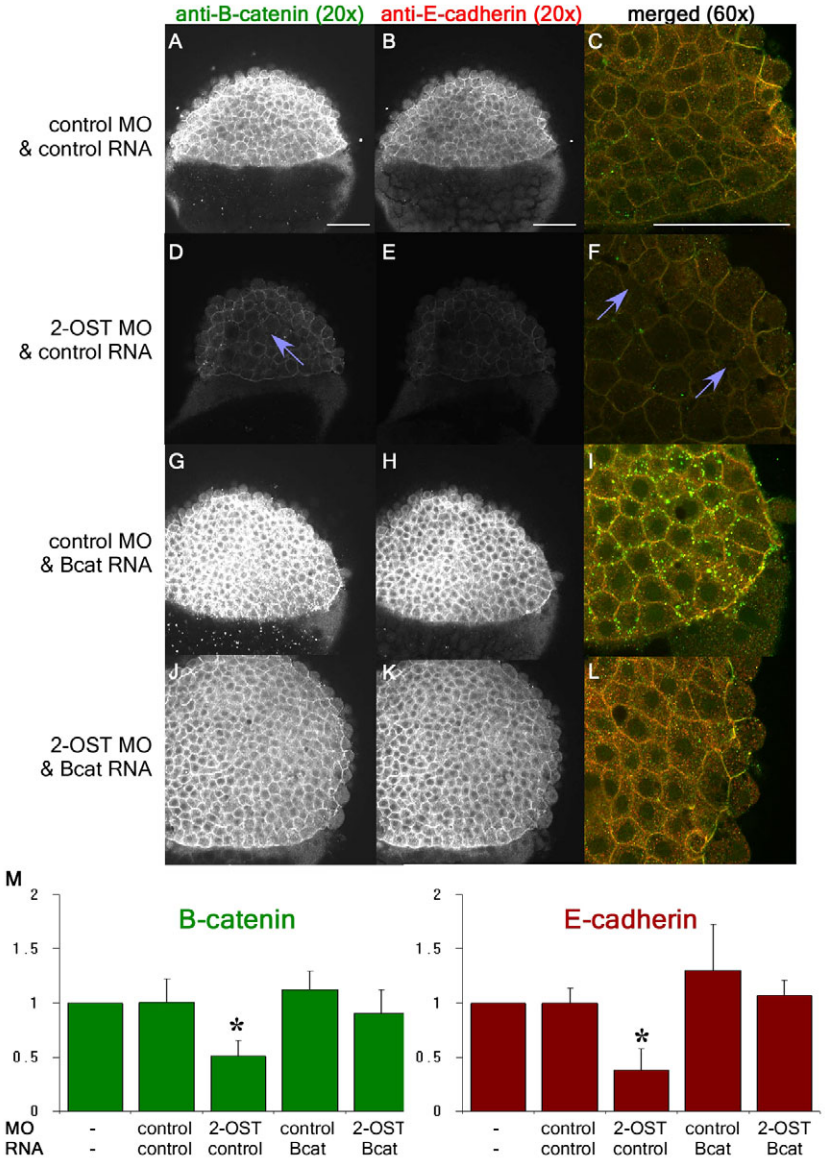

Fig. 4. β-Catenin accumulation is dependent on 2-OST. (**A**,**D**,**G**,**J**) Single planes of *z*-stack at 4 hpf of β-catenin for control MO+control RNA- (A), 2-OST MO+control RNA- (D), control MO+stabilized β-*catenin* RNA- (G), and 2-OST MO+stabilized β-*catenin* RNA (J)-injected embryos. (**B**,**E**,**H**,**K**) Single planes of *z*-stack of E-cadherin control MO+ control RNA- (B), 2-OST MO+control RNA- (E), control MO +stabilized β-*catenin* RNA- (H), and 2-OST MO+stabilized β-*catenin* RNA (K)-injected embryos. (**C**,**F**,**I**,**L**) Merged images of β-catenin and E-cadherin for control MO+control RNA (C), 2-OST MO+control RNA- (F), control MO+stabilized β-*catenin* RNA- (I), and 2-OST MO +stabilized β-*catenin* RNA (L)-injected embryos (*n*=21 for each group). The purple arrows indicate regions in which adhesion is completely lost between deep cells based on dark spaces and altered cellular morphology. Scale bars: 100 μm. (**M**) Western blot results, comparing band densitometry at 4 hpf. β-*catenin* (green) levels per sample were normalized to α-tubulin levels per sample, and then WT, control MO and control RNA, 2-OST MO and control RNA, control MO and stabilized β-*catenin* RNA, and 2-OST MO and stabilized β-*catenin* RNA were each normalized to WT, using WT as a value of 1. The same was done for the E-cadherin (red) (two embryos/lane/sample, *n*=5 experiments). **P*<0.05 for levels of protein statistically significantly different for the 2-OST MO and control RNA compared with all the other samples on the chart. Error bars represent s.d.

ost RNA along with the 2-OST MO (supplementary material Fig. S1G-I). Together, these results indicated that adherens junction proteins E-cadherin and β-catenin were reduced in 2-OST morphant deep cells, concurrent with a loss of cell-cell adhesion and the failure to initiate epiboly.

2-OST morphant adhesion defects can be rescued by β-catenin

We addressed next whether restoring the levels of β-catenin could rescue the adhesion defects in 2-OST morphants. We co-injected mRNA encoding a stabilized β-catenin, which cannot be targeted for degradation by the destruction complex (Dorsky et al., 2002), and examined protein localization, protein levels and cell morphologies at 4 hpf. Co-injection of stabilized β-*catenin* and control MO resulted in increased intensity for both β-catenin (Fig. 4G,I) and E-cadherin (Fig. 4H,I) at the cell membrane. Similarly, co-injection of stabilized β-*catenin* with 2-OST morpholino increased the levels of β-catenin (Fig. 4J,L) and E-cadherin (Fig. 4K,L) at the cell membrane, compared with the lower levels seen in 2-OST morphants injected with control mRNA (Fig. 4D-F). These increased levels of β-catenin and E-cadherin in both the control morphants and 2-OST morphants were confirmed by western analysis on 4 hpf embryos (Fig. 4M). The 2-OST morphant co-injected with the stabilized β-*catenin* resulted in levels of β-catenin and E-cadherin that are statistically significantly different than those observed following injection of the 2-OST morphant alone. Strikingly, injection of β-*catenin* mRNA in 2-OST morphants rescued the adhesion defects between the deep cells, abolishing the gaps between the deep cells, and rescued cell morphology back to normal.

2-OST-dependent levels of active β-catenin and transcriptional responses

To examine whether the effects of 2-OST upon the Wnt pathway are mediated by changes in β-catenin protein stability or by changes in the rate of transcription, we used two different approaches. We first examined the levels of the activated form of β-catenin by western blot using an antibody which recognizes the non-phosphorylated Ser37 and Thr41 epitope, and thus the active form of β-catenin. We observed that the levels of activated β-catenin are reduced in 2-OST morphants compared with the WT and control morphants (Fig. 5A). Using polyacrylamide gels that allowed us to distinguish by size between the activated endogenous β-catenin and the stabilized and activated exogenous β-catenin expressed by RNA injection (which is larger owing to a Myc-epitope tag), we found that expression of the exogenous stabilized β-catenin was capable of returning the total levels of activated β-catenin in the 2-OST morphants to approximately the same level of activated β-catenin observed in the WT.

Second, to examine whether the reduced levels of activated endogenous β-catenin in 2-OST morphants affects expression of Wnt-response genes, we used TOP-dGFP transgenic fish carrying a Wnt reporter that is transcriptionally active in the presence of stabilized β-catenin and Lef/Tcf proteins (Dorsky et al., 2002). Owing to the low levels of GFP expression in this reporter at 4 hpf, we had to measure reporter levels by quantitative rtPCR. As no Wnt targets have been successfully validated at this early stage in development, we also examined the levels of genes thought to be Wnt targets later in development (Shinya et al., 2000; Weidinger et al., 2005). To validate these targets, we examined not only the levels in the WT, control, and 2-OST morphants, but we also examined the levels when we co-injected the stabilized β-*catenin* RNA with 2-OST MO, presuming that if no change in transcriptional response was observed, then the gene was not a Wnt-responsive target gene at this stage of development. We observed that the levels of *axin2* and *dkk1b* along with the TOP-dGFP all responded to the stabilized β-*catenin*, leading us to conclude that they are relevant targets for this assay (Fig. 5B).

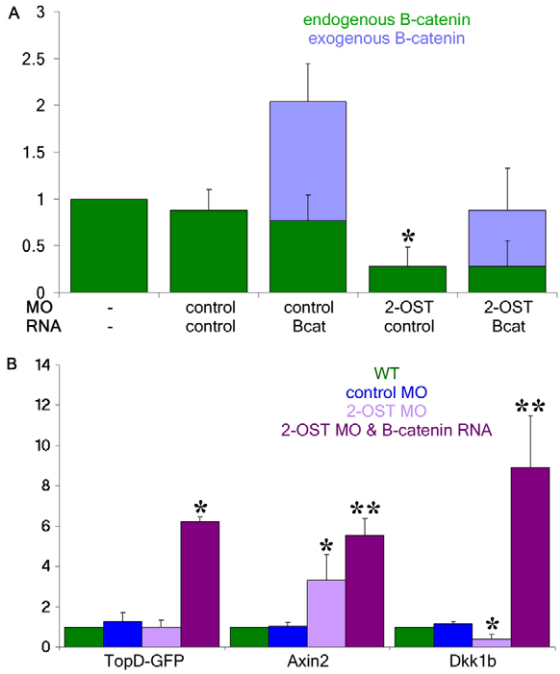

Fig. 5. 2-OST modulates active β-catenin protein, but not transcriptional responses. (**A**) Western blot for antibody against the active form of β-catenin at 4 hpf reveals that levels of active β-catenin were decreased in 2-OST morphants compared with wild type and control morphant (**P*<0.05) but total levels of active β-catenin were restored when 2-OST MO was co-injected with the stabilized β-*catenin* RNA. Levels were normalized to WT relative to levels of α-tubulin for each sample (two embryos/lane/sample, *n*=4 experiments). (**B**) qPCR for EGFP transcript in TOP-dGFP fish as well as *axin2* and *dkk1b*, which encode Wnt transcriptional targets, normalized to WT levels, analyzed using ΔΔcT method. *y*-axis indicates fold difference (combined data from *n*=8 series of experiments; **P*<0.05 from WT and control MO, ***P*<0.05 from WT, control MO, and 2-OST MO). Error bars represent s.d.

We observed no change in *TOP-dGFP* activity between the WT, control MO, and 2-OST MO embryos. Surprisingly, we observed an increase in *axin2* transcription in the 2-OST morphants compared with the controls, and a decrease in *dkk1b* in the 2-OST MO compared with the controls (Fig. 5B). We therefore speculate that small fluctuations in specific Wnt/β-catenin transcriptional targets might occur, perhaps owing to feedback pathways, but that major transcriptional changes, as indicated by the TOP-dGFP promoter, are not occurring in the 2-OST morphants at these early stages of development. This makes it likely that the decrease in the pool of β-catenin protein in 2-OST morphants has its strongest effects on functions at the cell membrane, not transcriptional regulation. Thus, we turned our attention back to the roles of 2-OST in the Wnt cytoplasmic response pathway.

2-OST modulates Wnt signaling upstream of Gsk3 and downstream of Wnt8

To examine whether the 2-OST-dependent regulation of the accumulation and cellular functions of β-catenin is dependent on the canonical Wnt cell-signaling pathway, epistasis experiments

were performed to test whether components of the Wnt pathway had effects on 2-OST morphants (Kelly et al., 1995). Wnt8 is a ligand that binds cell surface receptors, initiating the canonical Wnt signaling pathway. Gsk3 is part of the intracellular destruction complex that promotes the degradation of β-catenin in the absence of Wnt signaling. Expressing a dominant-negative Gsk3 (dnGSK3) protein interferes with the destruction complex, preventing the degradation of β-catenin and, thus, stabilizing its intracellular levels and simulating Wnt signaling.

The ectopic expression of Wnt8 increased the levels of β-catenin and E-cadherin in control morphants (Fig. 6G,H) such that it exceeded the levels in embryos co-injected with control RNA and control MO (Fig. 6A,B) and WT (supplementary material Fig. S2B). This indicates that Wnt8 is capable of activating the downstream Wnt response pathway in embryonic deep cells. Similarly, the expression of a dnGSK3 protein increased the levels of β-catenin and E-cadherin in control morphants (Fig. 6M,N), suggesting that this component of the intracellular Wnt signaling pathway is responsive in embryonic deep cells. Strikingly, the ability of Wnt8 to increase the levels of β-catenin and E-cadherin was blocked in 2-OST morphants. Wnt8 overexpression did not rescue the adhesion defects (Fig. 6J,K) in the embryonic deep cells of 2-OST morphants. By contrast, co-injection of dnGSK3 in 2-OST morphants rescued β-catenin and E-cadherin protein levels (Fig. 6P,Q). Together, the results of these epistasis experiments suggest that 2-OST functions downstream of the activity of the Wnt ligands but upstream of the destruction complex for β-catenin.

2-OST morphants exhibit reduced rates of proliferation that can be rescued by β-catenin

Cells are actively dividing at blastula stages of development, and disruptions in proliferation can result in epiboly defects (Kimmel et al., 1995; Rozario et al., 2009). In addition to its role in modulating adhesion, β-catenin contributes to the regulation of cell proliferation (Bienz, 2005; Brembeck et al., 2006). To address the question of whether reduced levels of β-catenin in 2-OST morphants were also affecting this classical aspect of β-catenin signaling, we measured the rates of cell proliferation by employing a BrdU incorporation assay (Aman et al., 2010). To determine the rate of proliferation, the total number of nuclei, indicated by the nuclear stain Sytox Green in a cross-section of the embryo (Fig. 7A,E), was compared with the number of cells that incorporated BrdU over a 20 minute period (Fig. 7C,G,K). The WT embryos and control morphants incorporated BrdU at the same rate, whereas only half the number of nuclei in 2-OST morphants had incorporated BrdU over the same time period (Fig. 7K).

As cell division in zebrafish embryos results in smaller cell volumes (Kimmel and Law, 1985a), if the rate of proliferation is reduced, the volumes of individual cells are predicted to be larger. Therefore, as a control study, average cell area was calculated from the total area of each embryo cross-section and the number of nuclei in that section. The average cross-sectional cell area of 2-OST morphants was larger than the control embryos (Fig. 7I). To test whether the 2-OST morphants were stalled during mitosis, an antibody against phospho-histone-3 (PH3; Fig. 7B,F,J) was used as a marker of M phase to determine the percentage of cells in M phase. The differences between the WT, control and 2-OST morphant embryos were not statistically significant (Fig. 7J).

We next sought to determine whether these cell cycle defects were dependent on altered β-catenin levels by assessing whether co-injection of the stabilized β-*catenin* could rescue the cell proliferation defect in 2-OST morphants. Co-injection of the stabilized *β-catenin* in 2-OST morphants significantly increased the cell proliferation rate, rescuing the 2-OST morphants back to normal cell proliferation rates (Fig. 7K). Stabilized β-*catenin* did not alter the normal proliferation rate in the control morphants (Fig. 7K). Together, results from cell morphology and cell cycle studies suggest that 2-OST acts upstream of β-catenin function to regulate the cell cycle.

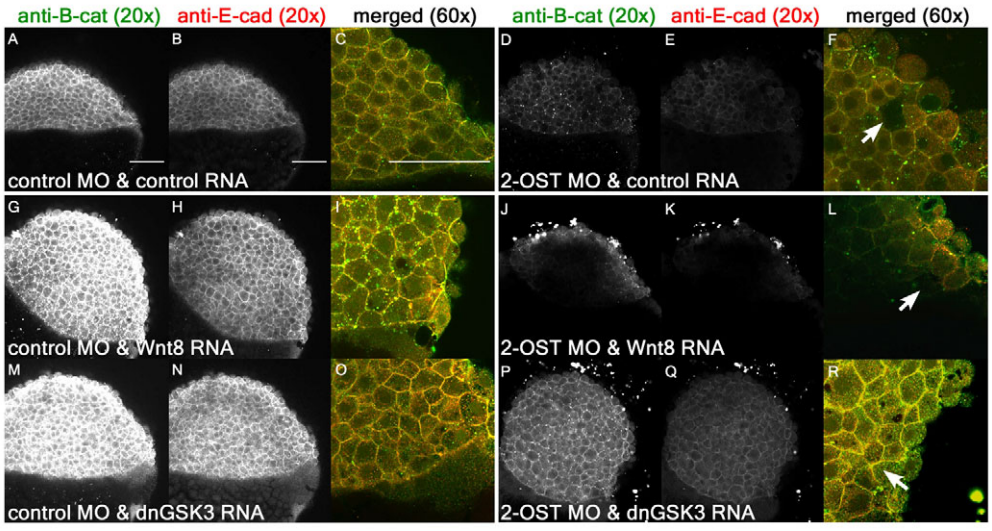

Fig. 6. 2-OST modulates Wnt signaling upstream of Gsk3 and downstream of Wnt8. (**A**,**D**,**G**,**J**,**M**,**P**) Single planes of *z*-stack at 4 hpf of β-catenin for control MO+control RNA- (A), 2-OST MO+control RNA- (D), control MO+Wnt8 RNA- (G), 2-OST MO+Wnt8 RNA- (J), control MO+dnGSK3 RNA- (M) and 2-OST MO+dnGSK3 RNA (P)-injected embryos. (**B**,**E**,**H**,**K**,**N**,**Q**) Cross-sections of E-cadherin for control MO+control RNA- (B), 2-OST MO+control RNA- (E), control MO+Wnt8 RNA- (H), 2-OST MO+Wnt8 RNA- (K), control MO+dnGSK3 RNA- (N) and 2-OST MO+dnGSK3 RNA (Q)-injected embryos. (**C**,**F**,**I**,**L**,**O**,**R**) Merged and magnified cross-sections of β-catenin and E-cadherin for control MO and control RNA- (C), 2-OST MO+control RNA- (F), control MO+Wnt8 RNA- (I), 2-OST MO+Wnt8 RNA- (L), control MO+dnGSK3 RNA- (O) and 2-OST MO+dnGSK3 RNA (R)-injected embryos. Arrows indicate regions in which adhesion is completely lost between deep cells based on dark spaces and altered cellular morphology. Scale bars: 100 μm.

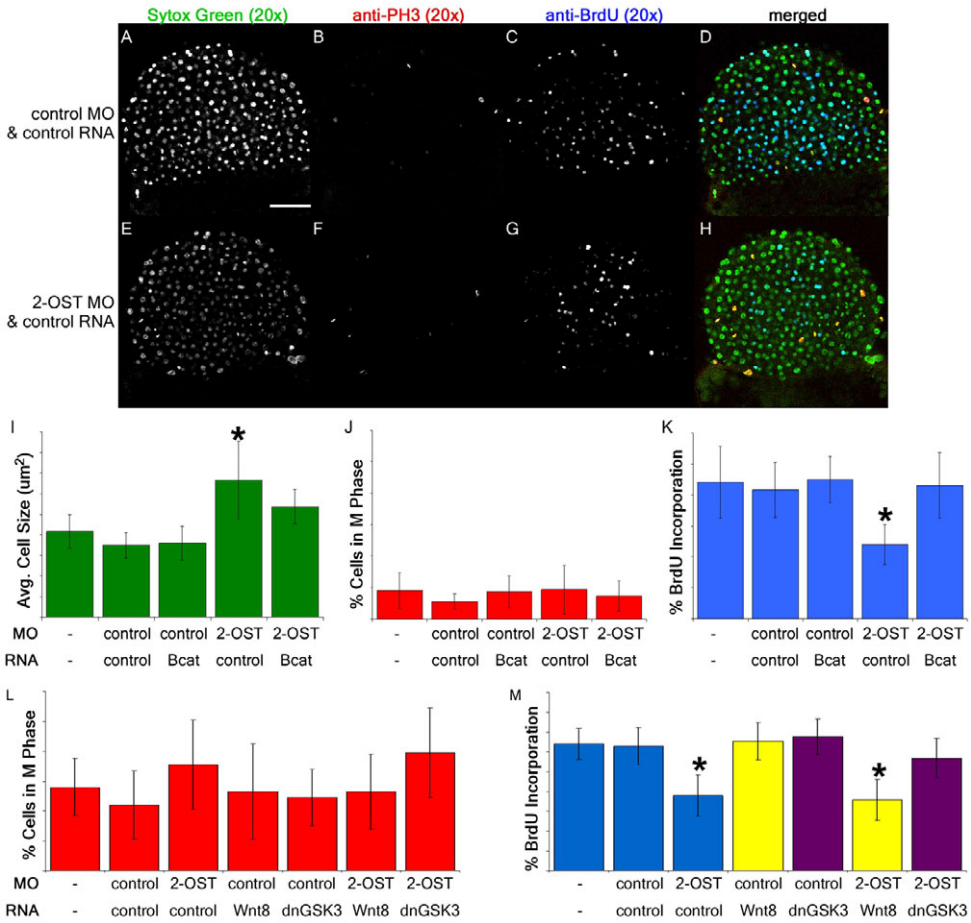

Fig. 7. 2-OST contributes to regulation of cell proliferation via β-catenin. (**A**,**E**) Single planes of *z*-stack of Sytox Green nuclear stain for control MO+control RNA- (A) and 2-OST MO+control RNA (E)-injected embryos. (**B**,**F**) Anti-phospho-histone H3 immunostaining of control MO+control RNA- (B) and 2-OST MO+control RNA (F)-injected embryos. (**C**,**G**) Anti-BrdU immunostaining of control MO+control RNA- (C) and 2-OST MO+control RNA (G)-injected embryos. (**D**,**H**) Merged images of Sytox Green, anti-phospho-histone-H3 and anti-BrdU staining of control MO+control RNA- (D) and 2-OST MO+control RNA (H)- injected embryos. Scale bar: 100 μm. (**I**) Comparison of average cell area. The cell area for 2-OST MO+control RNA-injected samples was statistically significantly different from all the other samples cell areas. (**J**) Comparison of percentage of cells in M phase. (**K**) Comparison of rate of cell proliferation. The rate of proliferation for 2-OST MO+control RNA-injected embryos was statistically significantly different from all the other samples rates of proliferation and was nearly half the rate of the controls. n=15 per group. (**L**) Comparison of percentage of cells in M phase. (**M**) Comparison of rate of proliferation. The rate of proliferation for the 2-OST MO+control RNA- and 2-OST MO+Wnt8 RNA-injected embryos was nearly half the rate of the controls (*n*=15 for each group). All these experiments were conducted at 4 hpf. **P*<0.05. Error bars represent s.d.

We applied the same series of epistasis parameters to our cell cycle BrdU incorporation experiments. Embryos injected with *wnt8* RNA and control MO, *dnGSK3* RNA and control MO, or control MO with control RNA, had levels of BrdU incorporation that were similar to those in uninjected WT embryos (Fig. 7M), indicating that higher levels of Wnt pathway activation are not capable of increasing the cell proliferation above its typical high rate in early embryos. Importantly, injection of *wnt8* RNA into 2-OST morphants did not rescue the cell proliferation defect back to the WT rate, resulting in the same lower rate seen in 2-OST morphants co-injected with control RNA. By contrast, when 2-OST MO was co-injected with the *dnGSK3* RNA, the rate of proliferation was rescued to a degree closely resembling the control levels. Together, results from these epistasis experiments suggest that 2-OST functions downstream of the activity of the Wnt ligands but upstream of the destruction complex for β-catenin in the regulation of cell cycle in zebrafish embryos.

DISCUSSION

This study reveals that 2-O-sulfation on HSPG GAG chains during vertebrate development is required for Wnt pathway-dependent cell adhesion and proliferation of embryonic deep cells and for the initiation of epiboly in zebrafish. Reducing the function of 2-OST results in an embryonic lethal phenotype caused by uncoupling cell adhesion and cell proliferation from the unperturbed processes of germ-layer specification and embryonic patterning.

The roles for β-catenin in vertebrate epiboly have not been explored. β-catenin interacts with E-cadherin to stabilize the adherens junctions that contribute to adhesive forces (Hammerschmidt and Wedlich, 2008; Lecuit and Lenne, 2007; Perez-Moreno and Fuchs, 2006; Perez-Moreno et al., 2003). Previous studies have demonstrated that E-cadherin is required for normal epiboly, promoting the thinning and spreading of the blastodisc as the less superficial deep cells intercalate with the more superficial cells of the blastodisc deep cell population. When E-cadherin levels are decreased, this process is disrupted. Here, we

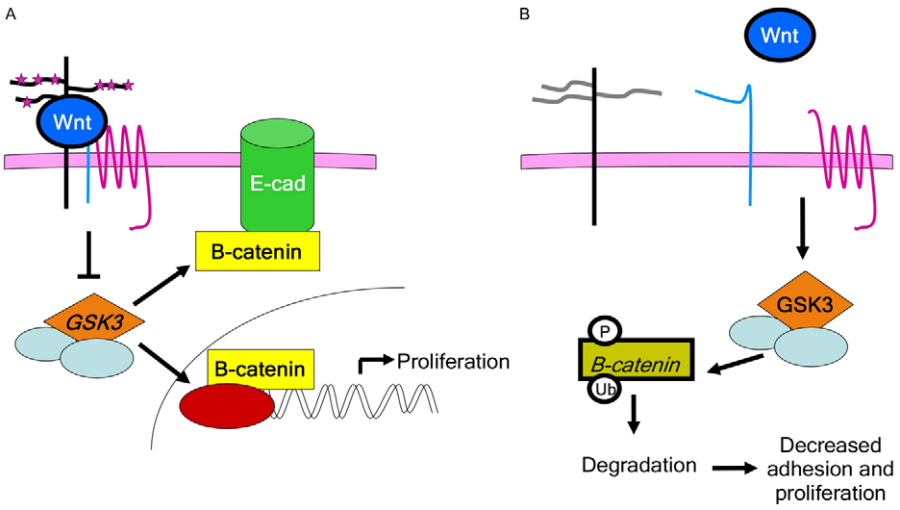

Fig. 8. Model for role of 2-O-sulfation in canonical Wnt signaling cascade. (**A**) Canonical Wnt signaling in the presence of 2-O-sulfation. 2-OST-dependent modifications (indicated by stars) on GAG chains of proteoglycans occur in the Golgi, before proteoglycans transit to the cell surface. These modifications are required for Wnt ligand function, upstream of intracellular components such as GSK3, for regulation of β-catenin levels, and cell junctional localization of β-catenin and E-cadherin (E-cad). (**B**) Wnt signaling in the absence of 2-O-sulfation. β-catenin levels are decreased, leading to decreased cell adhesion and decreased cell proliferation. P, phosphorylation; Ub, ubiquitin.

show that endogenous, active β-catenin protein levels are reduced in 2-OST morphants, suggesting that the cell adhesion defects in 2-OST morphants are due to a combined reduction of β-catenin and E-cadherin at the cell junctions in the deep cells. Strikingly, when stabilized β-catenin or DN-GSK3 are expressed in 2-OST morphants, the E-cadherin levels and adhesion are restored, suggesting that the level of β-catenin at the membrane regulates E-cadherin and adhesion in deep cells. By contrast, expression of Wnt8, a secreted extracellular ligand that activates the canonical Wnt cascade, increases levels of β-catenin in control MO embryos but fails to increase cell membrane localization of β-catenin or E-cadherin in 2-OST morphants, thus failing to rescue the cell adhesion defects (Fig. 8).

The 2-OST morphants had a decreased rate of cell proliferation, based on BrdU labeling, but did not display an increased level of Histone H3 phosphorylation, suggesting that cell cycle slowing or stalling occurred in a non-M phase part of the cell cycle. Epistasis results with *Wnt8* and *dnGSK3* RNA further supported our hypothesis that 2-OST functions in the Wnt signaling pathway downstream of ligand signaling and upstream of GSK3β activity, as cell proliferation in 2-OST morphants can be rescued by dnGSK3 but not by Wnt8.

Studies of Wnt signaling often focus on transcriptional regulation. Based on our observation that expression of the Wnt-responsive transgenic TOP-dGFP reporter is not altered in 2-OST morphants at the initiation of epiboly, and that other post-zygotic markers for germ layer and axis specification are expressed, we propose that the predominant role of 2-OST in the Wnt pathway is not based on transcriptional regulation, but on post-transcriptional control of steady-state levels of β-catenin or E-cadherin that are required for cell adhesion and cell cycle regulation. Given that the adhesion and epiboly phenotypes manifest shortly after the initiation of zygotic transcription, and that Wnt signaling during development and homeostasis appears to be more complex than simply ‘on’ or ‘off’ states (Kofron et al., 2007), our proposal that 2-OST regulates the post-transcriptional steady-state of the Wnt pathway is parsimonious.

Although reactivating the canonical Wnt cascade rescues the defects in cell proliferation and adhesion in 2-OST morphants, it fails to rescue the epiboly initiation defect. This is likely because the heparan sulfate GAG modifications driven by 2-OST control not only Wnt signaling pathways but other pathways as well, predicting that the epiboly defect is a compound phenotype of defective Wnt pathway-dependent cell adhesion and proliferation of embryonic deep cells, as well as Wnt-independent pathways that cannot be rescued by stabilization of β-catenin protein levels. This is in keeping with the observation that morpholino knockdown of β-catenin in zebrafish results in later developmental defects (Bellipanni et al., 2006), suggesting that maternally encoded β-*catenin* mRNA and accumulated β-catenin protein in the early embryo is sufficient for earlier processes such as cell adhesion and epiboly. The process of epiboly is controlled by several different components of the cytoskeleton in the yolk in addition to the intercalation and spreading of embryonic deep cells manipulated here (Cheng et al., 2004; Solnica-Krezel and Driever, 1994; Strahle and Jesuthasan, 1993; Zalik et al., 1999). However, the genes which regulate the yolk cytoplasmic processes are only beginning to identified and understood in a context of signaling cascades. Future studies will address roles that other possible signaling cascades might play in regulating epiboly and how the absence of 2-O-sulfation is modifying them.

Acknowledgements
We thank A. Cadwallader for initial characterization of 2-OST expression and morpholinos; J. Neugebauer and K. Ullman for critical reading of the manuscript; R. Dorsky for discussions of Wnt signaling, plasmids and a transgenic line; M. Vetter for a plasmid; R. Lawrence and J. Esko for discussions of metabolic labeling and attempts at GAG structural analysis.

Funding
This research was funded by grants from the National Institutes of Health [R01 NS48382 to M.L.C. and R01 HL66292 to H.J.Y.]. Deposited in PMC for release after 12 months.

Competing interests statement
The authors declare no competing financial interests.

Supplementary material
Supplementary material available online at
http://dev.biologists.org/lookup/suppl/doi:10.1242/dev.078238/-/DC1

References
Adachi, T., Sato, C., Kishi, Y., Totani, K., Murata, T., Usui, T. and Kitajima, K. (2009). Membrane microdomains from early gastrula embryos of medaka, Oryzias latipes, are a platform of E-cadherin- and carbohydrate-mediated cell-cell interactions during epiboly. *Glycoconj. J.* **26**, 285-299.
Aman, A., Nguyen, M. and Piotrowski, T. (2010). Wnt/beta-catenin dependent cell proliferation underlies segmented lateral line morphogenesis. *Dev. Biol.* **349**, 470-482.
Babb, S. G. and Marrs, J. A. (2004). E-cadherin regulates cell movements and tissue formation in early zebrafish embryos. *Dev. Dyn.* **230**, 263-277.

Bellipanni, G., Varga, M., Maegawa, S., Imai, Y., Kelly, C., Myers, A. P., Chu, F., Talbot, W. S. and Weinberg, E. S. (2006). Essential and opposing roles of zebrafish beta-catenins in the formation of dorsal axial structures and neurectoderm. *Development* **133**, 1299-1309.
Betchaku, T. and Trinkaus, J. P. (1978). Contact relations, surface activity, and cortical microfilaments of marginal cells of the enveloping layer and of the yolk syncytial and yolk cytoplasmic layers of fundulus before and during epiboly. *J. Exp. Zool.* **206**, 381-426.
Bienz, M. (2005). beta-Catenin: a pivot between cell adhesion and Wnt signalling. *Curr. Biol.* **15**, R64-R67.
Bink, R. J., Habuchi, H., Lele, Z., Dolk, E., Joore, J., Rauch, G. J., Geisler, R., Wilson, S. W., den Hertog, J., Kimata, K. et al. (2003). Heparan sulfate 6-o-sulfotransferase is essential for muscle development in zebrafish. *J. Biol. Chem.* **278**, 31118-31127.
Brembeck, F. H., Rosario, M. and Birchmeier, W. (2006). Balancing cell adhesion and Wnt signaling, the key role of beta-catenin. *Curr. Opin. Genet. Dev.* **16**, 51-59.
Bullock, S. L., Fletcher, J. M., Beddington, R. S. and Wilson, V. A. (1998). Renal agenesis in mice homozygous for a gene trap mutation in the gene encoding heparan sulfate 2-sulfotransferase. *Genes Dev.* **12**, 1894-1906.
Cadwallader, A. B. and Yost, H. J. (2007). Combinatorial expression patterns of heparan sulfate sulfotransferases in zebrafish: III. 2-O-sulfotransferase and C5-epimerases. *Dev. Dyn.* **236**, 581-586.
Cheng, J. C., Miller, A. L. and Webb, S. E. (2004). Organization and function of microfilaments during late epiboly in zebrafish embryos. *Dev. Dyn.* **231**, 313-323.
Dorsky, R. I., Sheldahl, L. C. and Moon, R. T. (2002). A transgenic Lef1/beta-catenin-dependent reporter is expressed in spatially restricted domains throughout zebrafish development. *Dev. Biol.* **241**, 229-237.
Du, S., Draper, B. W., Mione, M., Moens, C. B. and Bruce, A. E. (2011). Differential regulation of epiboly initiation and progression by zebrafish Eomesodermin A. *Dev. Biol*. **362**, 11-23.
Esko, J. D. and Selleck, S. B. (2002). Order out of chaos: assembly of ligand binding sites in heparan sulfate. *Annu. Rev. Biochem.* **71**, 435-471.
Essner, J. J., Branford, W. W., Zhang, J. and Yost, H. J. (2000). Mesendoderm and left-right brain, heart and gut development are differentially regulated by pitx2 isoforms. *Development* **127**, 1081-1093.
Essner, J. J., Amack, J. D., Nyholm, M. K., Harris, E. B. and Yost, H. J. (2005). Kupffer's vesicle is a ciliated organ of asymmetry in the zebrafish embryo that initiates left-right development of the brain, heart and gut. *Development* **132**, 1247-1260.
Fujita, K., Takechi, E., Sakamoto, N., Sumiyoshi, N., Izumi, S., Miyamoto, T., Matsuura, S., Tsurugaya, T., Akasaka, K. and Yamamoto, T. (2010). HpSulf, a heparan sulfate 6-O-endosulfatase, is involved in the regulation of VEGF signaling during sea urchin development. *Mech. Dev.* **127**, 235-245.
Gotte, M., Spillmann, D., Yip, G. W., Versteeg, E., Echtermeyer, F. G., van Kuppevelt, T. H. and Kiesel, L. (2008). Changes in heparan sulfate are associated with delayed wound repair, altered cell migration, adhesion and contractility in the galactosyltransferase I (beta4GalT-7) deficient form of Ehlers-Danlos syndrome. *Hum. Mol. Genet.* **17**, 996-1009.
Habuchi, H., Nagai, N., Sugaya, N., Atsumi, F., Stevens, R. L. and Kimata, K. (2007). Mice deficient in heparan sulfate 6-O-sulfotransferase-1 exhibit defective heparan sulfate biosynthesis, abnormal placentation, and late embryonic lethality. *J. Biol. Chem.* **282**, 15578-15588.
Hacker, U., Nybakken, K. and Perrimon, N. (2005). Heparan sulphate proteoglycans: the sweet side of development. *Nat. Rev. Mol. Cell Biol.* **6**, 530-541.
Hammerschmidt, M. and Wedlich, D. (2008). Regulated adhesion as a driving force of gastrulation movements. *Development* **135**, 3625-3641.
Kamimura, K., Rhodes, J. M., Ueda, R., McNeely, M., Shukla, D., Kimata, K., Spear, P. G., Shworak, N. W. and Nakato, H. (2004). Regulation of Notch signaling by Drosophila heparan sulfate 3-O sulfotransferase. *J. Cell Biol.* **166**, 1069-1079.
Kane, D. and Adams, R. (2002). Life at the edge: epiboly and involution in the zebrafish. *Results Probl. Cell Differ.* **40**, 117-135.
Kane, D. A., McFarland, K. N. and Warga, R. M. (2005). Mutations in half baked/E-cadherin block cell behaviors that are necessary for teleost epiboly. *Development* **132**, 1105-1116.
Kelly, G. M., Erezyilmaz, D. F. and Moon, R. T. (1995). Induction of a secondary embryonic axis in zebrafish occurs following the overexpression of beta-catenin. *Mech. Dev.* **53**, 261-273.
Kimmel, C. B. and Law, R. D. (1985a). Cell lineage of zebrafish blastomeres. I. Cleavage pattern and cytoplasmic bridges between cells. *Dev. Biol.* **108**, 78-85.
Kimmel, C. B. and Law, R. D. (1985b). Cell lineage of zebrafish blastomeres. III. Clonal analyses of the blastula and gastrula stages. *Dev. Biol.* **108**, 94-101.
Kimmel, C. B., Ballard, W. W., Kimmel, S. R., Ullmann, B. and Schilling, T. F. (1995). Stages of embryonic development of the zebrafish. *Dev. Dyn.* **203**, 253-310.
Kinnunen, T., Huang, Z., Townsend, J., Gatdula, M. M., Brown, J. R., Esko, J. D. and Turnbull, J. E. (2005). Heparan 2-O-sulfotransferase, hst-2, is essential for normal cell migration in Caenorhabditis elegans. *Proc. Natl. Acad. Sci. USA* **102**, 1507-1512.
Kofron, M., Birsoy, B., Houston, D., Tao, Q., Wylie, C. and Heasman, J. (2007). Wnt11/beta-catenin signaling in both oocytes and early embryos acts through LRP6-mediated regulation of axin. *Development* **134**, 503-513.
Lamanna, W. C., Kalus, I., Padva, M., Baldwin, R. J., Merry, C. L. and Dierks, T. (2007). The heparanome-the enigma of encoding and decoding heparan sulfate sulfation. *J. Biotechnol.* **129**, 290-307.
Lawrence, R., Olson, S. K., Steele, R. E., Wang, L., Warrior, R., Cummings, R. D. and Esko, J. D. (2008). Evolutionary differences in glycosaminoglycan fine structure detected by quantitative glycan reductive isotope labeling. *J. Biol. Chem.* **283**, 33674-33684.
Lecuit, T. and Lenne, P. F. (2007). Cell surface mechanics and the control of cell shape, tissue patterns and morphogenesis. *Nat. Rev. Mol. Cell Biol.* **8**, 633-644.
Link, V., Shevchenko, A. and Heisenberg, C. P. (2006). Proteomics of early zebrafish embryos. *BMC Dev. Biol.* **6**, 1.
Perez-Moreno, M. and Fuchs, E. (2006). Catenins: keeping cells from getting their signals crossed. *Dev. Cell* **11**, 601-612.
Perez-Moreno, M., Jamora, C. and Fuchs, E. (2003). Sticky business: orchestrating cellular signals at adherens junctions. *Cell* **112**, 535-548.
Reijmers, R. M., Vondenhoff, M. F., Roozendaal, R., Kuil, A., Li, J. P., Spaargaren, M., Pals, S. T. and Mebius, R. E. (2010). Impaired lymphoid organ development in mice lacking the heparan sulfate modifying enzyme glucuronyl C5-epimerase. *J. Immunol.* **184**, 3656-3664.
Reim, G. and Brand, M. (2006). Maternal control of vertebrate dorsoventral axis formation and epiboly by the POU domain protein Spg/Pou2/Oct4. *Development* **133**, 2757-2770.
Rohde, L. A. and Heisenberg, C. P. (2007). Zebrafish gastrulation: cell movements, signals, and mechanisms. *Int. Rev. Cytol.* **261**, 159-192.
Rozario, T., Dzamba, B., Weber, G. F., Davidson, L. A. and DeSimone, D. W. (2009). The physical state of fibronectin matrix differentially regulates morphogenetic movements in vivo. *Dev. Biol.* **327**, 386-398.
Shinya, M., Eschbach, C., Clark, M., Lehrach, H. and Furutani-Seiki, M. (2000). Zebrafish Dkk1, induced by the pre-MBT Wnt signaling, is secreted from the prechordal plate and patterns the anterior neural plate. *Mech. Dev.* **98**, 3-17.
Solnica-Krezel, L. and Driever, W. (1994). Microtubule arrays of the zebrafish yolk cell: organization and function during epiboly. *Development* **120**, 2443-2455.
Strahle, U. and Jesuthasan, S. (1993). Ultraviolet irradiation impairs epiboly in zebrafish embryos: evidence for a microtubule-dependent mechanism of epiboly. *Development* **119**, 909-919.
Walsh, E. C. and Stainier, D. Y. (2001). UDP-glucose dehydrogenase required for cardiac valve formation in zebrafish. *Science* **293**, 1670-1673.
Weidinger, G., Thorpe, C. J., Wuennenberg-Stapleton, K., Ngai, J. and Moon, R. T. (2005). The Sp1-related transcription factors sp5 and sp5-like act downstream of Wnt/beta-catenin signaling in mesoderm and neuroectoderm patterning. *Curr. Biol.* **15**, 489-500.
Westerfield, M. (1993). *The Zebrafish Book: A Guide for the Laboratory Use of Zebrafish (Brachydanio rerio).* Eugene, OR: M. Westerfield.
Zalik, S. E., Lewandowski, E., Kam, Z. and Geiger, B. (1999). Cell adhesion and the actin cytoskeleton of the enveloping layer in the zebrafish embryo during epiboly. *Biochem. Cell Biol.* **77**, 527-542.